HHS Public Access

Author manuscript

Dig Dis Sci. Author manuscript; available in PMC 2019 February 01.

Published in final edited form as:

Dig Dis Sci. 2018 February ; 63(2): 356–365. doi:10.1007/s10620-017-4867-5.

Apical membrane alterations in non-intestinal organs in Microvillus Inclusion Disease

Cameron Schlegel[1,3,+], **Victoria G. Weis**[1,3,+], **Byron C. Knowles**[2,3,+], **Lynne A. Lapierre**[1,3], **Martin G. Martin**[4], **Paul Dickman**[6], **James R. Goldenring**[1,2,3,*], and **Mitchell D. Shub**[5]

[1]Departments of Surgery, Vanderbilt University School of Medicine, Nashville, TN, USA

[2]Cell & Developmental Biology, Vanderbilt University School of Medicine, Nashville, TN, USA

[3]Epithelial Biology Center, Vanderbilt University School of Medicine, Nashville, TN, USA

[4]Department of Pediatrics, Division of Gastroenterology and Nutrition, Mattel Children's Hospital, David Geffen School of Medicine, University of California Los Angeles, Los Angeles, CA, USA

[5]Division of Gastroenterology, Phoenix Children's Hospital and the Department of Child Health, University of Arizona College of Medicine-Phoenix, Phoenix, AZ, USA

[6]Pathology and Laboratory Medicine, Phoenix Children's Hospital and the Department of Child Health, University of Arizona College of Medicine-Phoenix, Phoenix, AZ, USA

Abstract

Objectives—Microvillus Inclusion Disease (MVID) is a severe form of neonatal diarrhea, caused mainly by mutations in *MYO5B*. Inactivating mutations in *MYO5B* causes depolarization of enterocytes in the small intestine, which gives rise to chronic, unremitting secretory diarrhea. While the pathology of the small intestine in MVID patients is well described, little is known about extraintestinal effects of MYO5B mutation.

Methods—We examined stomach, liver, pancreas, colon and kidney in Navajo MVID patients, who share a single homozygous *MYO5B-P660L* (1979C>T p.Pro660Leu, exon 16). Sections were stained for markers of the apical membrane to assess polarized trafficking.

Results—Navajo MVID patients showed notable changes in H/K-ATPase-containing tubulovesicle structure in the stomach parietal cells. Colonic mucosa was morphologically normal, but did show losses in apical ezrin and Syntaxin 3. Hepatocytes in the MVID patients displayed aberrant canalicular expression of the essential transporters MRP2 and BSEP. The pancreas showed small fragmented islets and a decrease in apical ezrin in pancreatic ducts. Kidney showed normal primary cilia.

[*]**Correspondence should be addressed to:** James R. Goldenring, M.D., Ph.D. Epithelial Biology Center Vanderbilt University Medical Center 10435 Medical Research Building IV 2213 Garland Avenue, Nashville, TN 37232, Phone: 615-936-3726, FAX: 615-343-1591, jim.goldenring@vanderbilt.edu.

[+]These authors contributed equally.

The authors have declared that no conflict of interest exists.

Conclusions—These findings indicate that the effects of the P660L mutation in MYO5B in Navajo MVID patients are not limited to the small intestine, but that certain tissues may be able to compensate functionally for alterations in apical trafficking.

Keywords

Rab11a; Myosin Vb; MYO5B; Syntaxin 3; primary cilium; Parietal cells; BSEP; Ezrin; MRP2

Introduction

Children with Microvillus Inclusion Disease (MVID) present with unremitting neonatal diarrhea and have generalized villus blunting, loss of polarity and microvilli, and pathognomonic intracellular microvillus inclusions in enterocytes of the small intestine (1, 2). Previous investigations have identified inactivating mutations in myosin Vb (MYO5B) as the cause for this disease (3, 4). MYO5B is expressed in all epithelial tissues, as a motor protein regulating membrane transport and membrane recycling in polarized cells (5). Because patients present with profound diarrhea, MVID research has justly focused on the enterocytes of the small intestine (6). Consequently, other highly polarized tissues have not been well examined in detail, despite the prominent role of the apical recycling system in establishing polarity and promoting proper function in these tissue types including the stomach, liver, pancreas, kidney and the large intestine.

In gastric parietal cells, regulated apical recycling is the primary pathway for movement of H/K-ATPase-containing tubulovesicles to the apical surface (7, 8). The parietal cell's main function is to pump protons (H^+) into the lumen of the stomach using H/K-ATPase at the apical plasma membrane (9). This function requires transitioning between two apical structural arrangements; resting and stimulated. In the resting state, the apical surface is elaborated into apical invaginations comprising the intracellular canaliculi, which represent an expanded apical plasma membrane supported by F-actin bundled with ezrin (10–12). Underneath the apical surface of the intracellular canaliculi, Rab11a-containing tubulovesicles harbor a resting pool of H/K-ATPase (7, 13). Upon stimulation, H/K-ATPase-containing tubulovesicles fuse into the apical canaliculi. Structural changes related to the stimulated configuration are associated with phosphorylation of ezrin and result in the formation of multiple microvillar extensions from the canalicular surface, which increase the apical availability of H/K-ATPase (8, 11, 14).

Similarly, both the liver and colon are highly polarized tissues that depend on apical vesicle trafficking for their normal function. Hepatocytes polarize into two distinct surfaces; one surface opens into bile canaliculi with sparse microvilli (apical), while the second surface faces sinusoidal capillaries (basolateral) (15). MYO5B-coupled Rab11a-dependent trafficking is required by apical ATP-binding-cassette (ABC) transporters to establish the apical surface in hepatocytes, and expression of dominant negative mutations in either Rab11a or MYO5B caused aberrant trafficking of ABC transporters, BSEP and MRP2 (16, 17). Interestingly, in enterocytes MYO5B interaction with Rab8a promotes the establishment of microvilli growth, and MYO5B interaction with Rab11a is required for apical recycling of membranes internalized through apical bulk endocytosis and also facilitates the maintenance

of microvilli in enterocytes (18). MYO5B has also been implicated in the recruitment to the apical surface of MST4 and atypical protein kinase C (aPKC), which are responsible for the phosphorylation of ezrin in enterocytes (19). Thus, Rab8a and Rab11a-dependent apical trafficking coupled to MYO5B facilitate proper trafficking in both hepatocytes and enterocytes (18, 20).

In the Navajo population, MVID has an incidence of 1 case per 12,000 live births, with a homozygous *MYO5B-P660L* (1979C>T p.Pro660Leu, exon 16) mutation, inherited in an autosomal recessive pattern, responsible for all cases (4, 21). In this report, we examined non-intestinal tissue samples from Navajo MVID patients. We report that MYO5B appears to alter the apical membrane composition in a number of epithelial organs, with altered tubulovesicular trafficking in the stomach, and disruption of apical and basolateral markers in the stomach and large intestine. These changes were also present in the liver, where these patients also appeared to display loss of MYO5B, with aberrant trafficking MRP2 and BSEP in the hepatocytes. In the pancreas fragmentation of Islets of Langerhans was observed along with alterations in apical ezrin in the pancreatic ducts. Nevertheless, the apical primary cilia in kidney epithelial cells appeared relatively unaffected. These findings suggest that the effects of MYO5B mutations in Navajo MVID patients are not tissue specific. Rather alterations in apical membrane trafficking are observed across many epithelial tissue types.

Materials and Methods

Study Approval and Tissue preparation

The studies in these investigations utilized archival paraffin tissue specimens from normal children and four Navajo MVID patients. All procedures and studies were performed according to protocols approved by Institutional Review Boards (IRB) at both Phoenix Children's Hospital and Vanderbilt University School of Medicine. IRB approval of informed consent was obtained from all families of living subjects prior to research and IRB approved decedent research on tissue blocks from patients who had expired.

One Navajo patient was transplanted at 9 months of age because of end stage liver disease and intestinal failure. The multivisceral transplant included segmental transplant of the liver (left lobe), stomach, pancreas, small intestine, and colon with an arterial interposition graft. Tissue samples from the Navajo patient were obtained from resected specimens that were obtained at the time of the transplantation following the family's signed IRB consent. Archival biopsies of the liver from one Navajo patient at 1 year and eleven months of age and biopsies from a third 18 day old Navajo patient from the stomach, liver and colon were also examined. We also examined stomach biopsies from a Navajo patient at 9 years of age and kidney biopsies from the same patient at 11 years of age. All reference controls were obtained from de-identified archival tissue samples obtained from the pathology archives at Vanderbilt University Medical Center. The reference colon sample was from a patient less than 1 year old. Other reference samples were from adults.

Histology

All biopsy and resection samples were prepared as detailed by Knowles, et al. 2014 (18). Normal human and MVID patient sections were de-paraffinized and were submitted to antigen retrieval in a pressure cooker using the Target Retrieval Solution (Dako North America Inc.). Serum free protein block (Dako North America Inc.) was used for blocking tissue, and sections were incubated overnight at 4°C with primary antibodies diluted in 1% normal donkey serum and 0.01% Tween-20 in PBS. Cells were washed three times for 15 minutes at room temperature with 0.01% Tween-20 in PBS (PBS-T). Appropriate secondary antibodies were conjugated for immunofluorescence with Alexa 488, Alexa 568, Alexa 647, Cy3, or Cy5 (1.5-hour incubation at room temperature). Detailed information on primary antibodies and their dilutions are listed in Table 1. Images were captured with an Olympus FV-1000 confocal microscope (Olympus, Toxyo, Japan) or Zeiss Axiophot microscope equipped with an Axiovision digital imaging system (Zeiss, Jena GmBH, Germany). The individual images were converted to tiff files with the FV-1000 software, and Photoshop (Adobe) was used to create the final figures.

Samples for structured illumination microscopy (SIM) were prepared as for confocal immunofluorescence (see above). SIM imaging was performed on a DeltaVision OMX microscope (Applied Precision Inc.) using 488 nm, 568 nm, and 642 nm lasers. Reconstruction and alignment of SIM images was performed using softWoRx version 5.0 (GE/Applied Precision Inc.). These corrections were applied back into the acquired images, and Adobe Photoshop was used to produce the final images.

Results

Inactivating P660L mutation of MYO5B caused altered morphology in parietal cells

Previous work has demonstrated that parietal cells depend on regulated Rab11a-dependent trafficking of H/K-ATPase containing tubulovesicle pools to the apical surface to pump H^+ into the lumen of the stomach (14). H/K-ATPase-containing tubulovesicles from parietal cells contain a wide array of apical trafficking proteins including: Rab11a, VAMP2, and STX3 (13, 22, 23). However, the role of MYO5B on these vesicles remains unclear. Since, MYO5B interacts directly with Rab11a to facilitate vesicle trafficking in other cell types, we reasoned that mutations in MYO5B might affect parietal cell function, because of their high levels of Rab11a (7, 14, 24). To examine the effects of the Navajo MYO5B mutation (*MYO5B-P660L*) on parietal cells in MVID patients, we immunostained stomach biopsy samples from two Navajo MVID patients for H/K-ATPase and ezrin. In normal stomach sections, immunostaining for ezrin and H/K-ATPase were associated with the apical canalicular region of parietal cells (Figure 1A). In contrast, MVID patient samples showed a marked concentration of H/K-ATPase staining in more compressed membrane structures in parietal cells and a reduction of ezrin staining and redistribution to the cytoplasm (Figure 1A). Similar results were observed in both MVID stomach samples. Structured illumination microscopy (SIM) of the MVID patient samples revealed aberrant intracellular localization of H/K-ATPase (Figure 1B). The localization of pepsinogen in chief cells and GSII lectin (reflective of Muc6-containing mucous granules) in mucous neck cells appeared to be unaffected in MVID patient stomach sections (Figure 2).

Normal function of parietal cells is dependent upon the establishment of electrochemical gradients and contact with neighboring cells. To evaluate the integrity of these systems in the basolateral compartment of the MVID patient stomach samples, we immunostained the stomach sections for phospho-ERM (pERM), p120 and Na/K-ATPase. In normal stomach sections, Na/K-ATPase and p120-catenin (p120) immunostaining was localized to the basolateral surface of parietal cells (Figure 1C). In contrast, MVID patient samples showed an increase in cytoplasmic staining for both Na/K-ATPase and p120, but generally maintained their basolateral distribution (Figure 1C). Interestingly, phosphorylated ERM (Ezrin, Radixin, Moesin) staining, generally reflective of phosphorylated ezrin in parietal cells in the stomach, appeared to be decreased and redistributed to the cytoplasm in MVID patient stomach sections, when compared to normal stomach sections (Figure 1C). These findings suggest that mutation of MYO5B in the Navajo MVID patients' stomach can alter normal apical canalicular trafficking in parietal cells.

P660L mutation of MYO5B causes loss of apical components in the colonocytes of the large intestine

MVID disrupts normal apical and basolateral polarity in the enterocytes of the small intestine (18). The colonocytes of the large intestine function to absorb water after initial digestion in the small intestine, but in the context of MVID the large intestine has not been studied extensively. To examine the effects of mutations in MYO5B on the large intestine, we immunostained MVID patient colon samples for Ezrin, Syntaxin 3, p120, E-cadherin, and claudin-2 (CLDN2). In general, the colonic mucosal height in the both MVID samples was less than in control colon tissue. In control colon samples, Ezrin and Syntaxin 3 were localized to the apical surface, yet in MVID patient colon samples, there was apparent loss of apical staining of both Ezrin and Syntaxin 3 (Figure 3A). Interestingly, phosphorylated ERM was reduced in both MVID patient samples, and both Rab8a and Rab11a were redistributed to the cytoplasm (data not shown). In both the control and MVID patient colon samples, p120, E-cadherin, and CLDN2 were all normally localized along the basolateral surface (Figure 3B). Thus, MYO5B mutations in colonocytes may affect apical distribution of proteins, but the basolateral compartment remains intact.

P660L MYO5B mutation leads to redistribution of BSEP and MRP2 in MVID patient liver samples

To investigate the effects of MYO5B mutations on the liver, we immunostained patient samples for the ATP-binding cassette transporters BSEP (Bile Salt Export Pump) and MRP2 (Multidrug Resistance-associated Protein 2). MVID patients often struggle with chronic cholestasis, and previous investigations noted that in MVID patient liver samples, proper trafficking of BSEP was disrupted, but MRP2 appeared to be unaffected (25). While many MVID patients require long-term parenteral nutrition, making the etiology of hepatic dysfunction difficult to discern, recent work in patients without diarrhea but carrying biallelic MYO5B mutations and presenting with hepatic dysfunction suggests this change in BSEP distribution may be associated with alterations in bile acids and cholestasis that is specific to MYO5B mutations regardless of parenteral nutrition toxicity (26). To better understand the effects of MYO5B mutation on Navajo MVID patient samples, we immunostained MVID liver samples for ezrin, p120, MYO5B, MRP2 and BSEP. In normal

liver sections, ezrin lined the bile canalicular surface (Figure 4A), while p120 marked the lateral borders of hepatocytes. In MVID patient liver sections, both ezrin and p120 were relocated to the cytoplasm (Figure 4A). In normal liver sections, both MRP2 and BSEP stain canalicular surfaces, but in the Navajo MVID patient sections both MRP2 and BSEP were distributed throughout the cytoplasm of hepatocytes (Figure 4B). Similar results were found in both Navajo MVID patient liver samples.

Functional MYO5B is required for proper morphology of the endocrine pancreas

We evaluated beta cells in an MVID patient's pancreas using immunohistochemistry for insulin. In normal pancreas sections, insulin staining was positive in beta cells of the Islets of Langerhans (Supplemental Figure 1A). In MVID patient pancreas sections, insulin staining demonstrated the presence of fragmented small collections of islet cells throughout the pancreas, but acinar cell mass was generally maintained (Supplemental Figure 1A). Additional evaluation of apical membrane integrity with ezrin staining demonstrated redistribution of ezrin from an apical localization in normal pancreatic ducts tissue to basolateral and cytoplasmic distribution in the MVID patient, while p120 demonstrated lateral staining in normal tissue, but was intracellular in the Navajo MVID patient (Supplemental Figure 1B). Loss of MYO5B was noted throughout the pancreas in the MVID patient.

The P660L MYO5B mutation does not appear to affect renal polarization

Primary cilia in the kidney are key components of renal sensing and adaptation, with increases in cilia length and changes in structure noted during times of injury and ischemia (27). Proteins are thought to be trafficked to the primary cilium utilizing elements of the endocytic recycling system, including Rab11a and Rab8a (28). Thus, we were interested in examining the affects of MYO5B mutation on primary cilia structure in renal MVID samples (Supplemental Figure 2). We evaluated renal primary cilia using antibodies against acetylated tubulin and Arl13b. Acetylated tubulin and Arl13b immunostaining demonstrated similar cilia structure and length in MVID patients compared to normal control kidney.

Discussion

Previous studies of MVID have focused on the impact of inactivating mutations in MYO5B on the polarity, morphology, and function of enterocytes of the small intestine (18). In this study, we evaluated the effects of mutations in MYO5B on the integrity of other organs in the gastrointestinal tract. Our investigations were limited by the small number of non-intestinal tissue samples available from Navajo MVID patients. Nevertheless, we found that the Navajo mutation of MYO5B does have significant effects on apical membrane protein expression in the stomach, liver, pancreas and colon. It should be noted that few of the MYO5B mutations have been characterized in detail. These mutations can range from early truncations that produce essentially MYO5B deletion, to point mutations predicted to alter either motor function or cargo binding. We have demonstrated that the P660L mutation in Navajo MVID patients leads to a motor that can bind actin, but cannot go through a motor stroke (a so-called rigor mutation) (18). Since the molecular consequences of other MYO5B mutations are not fully delineated, it is not clear whether other MYO5B mutations will elicit

the same impacts in non-intestinal tissues. Thus, our findings should not be considered definitive for non-intestinal phenotypes in other MVID MYO5B mutations.

In the Navajo MVID patient gastric parietal cells, H/K-ATPase was abnormally distributed intracellularly and did not associate with the intracellular canaliculi. In stomach samples, Na/K-ATPase was partially redistributed to the cytoplasm, and phosphorylated ERM proteins were markedly decreased. The apical recycling endosome (ARE) acts as the central decision point for both the biosynthetic and endocytic recycling pathways as they traffic and recycle proteins and lipids to and from the apical plasma membrane. Through its interactions with Rab8a and Rab11a, MYO5B plays a crucial role in apical membrane recycling (18, 24). Thus, it is not surprising that mutation of MYO5B would lead to altered trafficking in stomach parietal cells, as these cells have the highest endogenous levels of Rab11a, which is critical for recycling of H/K-ATPase-containing tubulovesicle membranes (7, 14, 29). Recently, MYO5B and Rab11a have been linked to ezrin phosphorylation in enterocytes, and we found a decrease in phosphorylated ERM member proteins in MVID patient stomach sections (19). Currently, it is not understood if phosphorylation of ezrin results in or is a consequence of the stimulated morphology in parietal cells. Interestingly, functional MYO5B loss in MVID patient parietal cells caused a reduction in apical ezrin similar to that observed in enterocytes (18).

In the MVID patient colon samples studied in this report, colonocytes showed loss of apical microvillar markers but interestingly no changes in claudin-2, E-cadherin, and p120. Notably, no microvillus inclusions were detected in enterocytes of the large intestine. The principle disease manifestation of MVID is chronic unremitting secretory and malabsorptive diarrhea. We have recently suggested that the pathophysiology of MVID is likely due to loss of apical trafficking and polarity that results from uncoupling of MYO5B from Rab8a and Rab11a (18). Deficits in apical functionality in the enterocytes of the colon may contribute to the clinical MVID phenotype, since the colon is unable to compensate for excess fluid secreted into the lumen of the small intestine.

In the liver samples examined in this report, hepatocytes contained intracellular ezrin, mislocalization of p120, and displayed aberrant intracellular localization of both MRP2 and BSEP. While it is often unclear whether the driving force behind hepatic failure in MVID patients is underlying genetic disease or parenteral nutrition associated hepatic failure, recent reports have found patients carrying biallelic MYO5B mutations with low γ-glutamyltransferase cholestasis without either diarrhea or parenteral nutrition, suggesting that further work is still needed to understand the underlying, intrinsic hepatic pathology in these patients (26). Our findings demonstrate mistrafficking of BSEP and MRP2, along with global changes in hepatocyte polarization with mislocalization of p120 and ezrin in Navajo MVID patient hepatocytes.

When examining the pancreas, we found abnormal small, fragmented Islets of Langerhans. It is not clear what this pattern fragmented islets connotes, but small and more numerous islets have been observed in monkeys with polycystic ovary disease, who are prone to developing diabetes (30). No clear predilection towards islet dysfunction has been reported with MYO5B mutation, although recently one 10 year old Navajo MVID patient was

reported to have developed diabetes (31). Although evidence of pancreatic beta cell dysfunction has yet to be documented widely in this population, the medical and nutritional complexities in these patients may foreshadow changes in pancreatic function that will merit further evaluation as these children live longer.

While prominent effects of MYO5B loss in MVID patients can be discerned in the gastrointestinal tract, few reports have indicated problems with kidney function. Nevertheless, previous investigations have suggested that both Rab11a and Rab8a are involved in establishment of the primary cilia in a number of cells (28, 32, 33). It was therefore of interest that we observed essentially normal primary cilia in biopsies from MVID patients. These results may suggest that Rab11a and Rab8a do not utilize MYO5B for trafficking to the primary cilium. Alternatively, since both Rab11a and Rab8a also can bind to MYO5A,(34) in the kidney Rab11a and Rab8a may use MYO5A for primary cilium formation or may act independent of MYO5 activities (35, 36).

In summary, our studies suggest that the loss of functional MYO5B does not simply result in intestinal pathology, but widely affects a variety of tissues in which the establishment and maintenance of apical polarity is crucial for organ specific function. Clearly, the functional impact of MYO5B inactivation is more penetrant in the small bowel and the liver. In the intestine, we have noted low levels of expression for MYO5A (37), a homologous motor protein that can associate with both Rab11a and Rab8a. Other organs which have higher levels of MYO5A, e.g. the kidney, may be able to compensate for a lack of MYO5B activity through the actions of MYO5A or through other mechanisms that may ameliorate any deficits in apical function. Nevertheless, as a number of MVID patients have received intestinal transplants over the past decade, it will be of interest to determine whether these patients will experience long-term effects of trafficking deficits in other organs. Further work is needed to better understand the clinical and physiological manifestations in these and other organs in MVID patients.

Supplementary Material

Refer to Web version on PubMed Central for supplementary material.

Acknowledgments

This work was supported by the NIH grant RO1 DK70856 and RO1 DK48370 to J.R.G and RAC Awards to M.S. from Phoenix Children’s Hospital for initial support of this project. V.G.S. and C.S. were supported by NIH Postdoctoral Fellowships (T32 DK007673). Confocal and structured illumination fluorescence microscopy imaging was performed through the use of the VUMC Cell Imaging Shared Resource and histological sectioning was performed by Translational Pathology Shared Resource, both supported by National Institute of Health (NIH) Grants CA68485, DK20593, DK58404 and HD15052. Fluorescence slide imaging was performed on an Ariol SL-50 digitizing scanner in the VUMC Digital Histology Shared Resource. We thank G. Silber, K. Ingebo, and D. Ursea for the outstanding care that they have provided over the years for the Navajo patients with MVID. We thank all of the families of our Navajo patients, who consented to allow archived tissue samples from their children to be used in this study.

References

1. Ruemmele FM, Schmitz J, Goulet O. Microvillous inclusion disease (microvillous atrophy). Orphanet J Rare Dis. 2006; 1:22. [PubMed: 16800870]

2. van der Velde KJ, Dhekne HS, Swertz MA, et al. An overview and online registry of microvillus inclusion disease patients and their MYO5B mutations. Hum Mutat. 2013; 34:1597–605. [PubMed: 24014347]

3. Muller T, Hess MW, Schiefermeier N, et al. MYO5B mutations cause microvillus inclusion disease and disrupt epithelial cell polarity. Nat Genet. 2008; 40:1163–5. [PubMed: 18724368]

4. Erickson RP, Larson-Thome K, Valenzuela RK, et al. Navajo microvillous inclusion disease is due to a mutation in MYO5B. Am J Med Genet A. 2008; 146A:3117–9. [PubMed: 19006234]

5. Rodriguez OC, Cheney RE. Human myosin-Vc is a novel class V myosin expressed in epithelial cells. J Cell Sci. 2002; 115:991–1004. [PubMed: 11870218]

6. Ameen NA, Salas PJ. Microvillus inclusion disease: a genetic defect affecting apical membrane protein traffic in intestinal epithelium. Traffic. 2000; 1:76–83. [PubMed: 11208062]

7. Goldenring JR, Soroka CJ, Shen KR, et al. Enrichment of rab11, a small GTP-binding protein, in gastric parietal cells. Am J Physiol. 1994; 267:G187–G194. [PubMed: 8074219]

8. Forte TM, Machen TE, Forte JG. Ultrastructural changes in oxyntic cells associated with secretory function: a membrane recycling hypothesis. Gastroenterology. 1977; 73:941–955. [PubMed: 902958]

9. Forte JG, Zhu L. Apical recycling of the gastric parietal cell H,K-ATPase. Annu Rev Physiol. 2010; 72:273–96. [PubMed: 20148676]

10. Ammar DA, Nguyen PN, Forte JG. Functionally distinct pools of actin in secretory cells. Am J Physiol. 2001; 281:C407–C417.

11. Hanzel D, Reggio H, Bretscher A, et al. The secretion-stimulated 80K phosphoprotein of parietal cells is ezrin, and has propoerties of a membrane cytoskeletal linker in the induced apical microvilli. EMBO J. 1991; 10:2363–2373. [PubMed: 1831124]

12. Hanzel D, Urushidani T, Usinger WR, et al. Immunological localization of an 80-kDa phosphoprotein to the apical membrane of gastric parietal cells. Am J Physiol. 1989; 256:G1082–G1089. [PubMed: 2472073]

13. Calhoun BC, Lapierre LA, Chew CS, et al. Rab11a redistributes to apical secretory canaliculus during stimulation of gastric parietal cells. Am J Physiol. 1998; 275:C163–C170. [PubMed: 9688847]

14. Duman JG, Tyagarajan K, Kolsi MS, et al. Expression of rab11a N124I in gastric parietal cells inhibits stimulatory recruitment of the H+-K+-ATPase. Am J Physiol. 1999; 277:C361–C372. [PubMed: 10484323]

15. Treyer A, Musch A. Hepatocyte polarity. Compr Physiol. 2013; 3:243–87. [PubMed: 23720287]

16. Wakabayashi Y, Dutt P, Lippincott-Schwartz J, et al. Rab11a and myosin Vb are required for bile canalicular formation in WIF-B9 cells. Proc Natl Acad Sci U S A. 2005; 102:15087–92. [PubMed: 16214890]

17. Wakabayashi Y, Lippincott-Schwartz J, Arias IM. Intracellular trafficking of bile salt export pump (ABCB11) in polarized hepatic cells: constitutive cycling between the canalicular membrane and rab11-positive endosomes. Mol Biol Cell. 2004; 15:3485–96. [PubMed: 15121884]

18. Knowles BC, Roland JT, Krishnan M, et al. Myosin Vb uncoupling from RAB8A and RAB11A elicits microvillus inclusion disease. J Clin Invest. 2014; 124:2947–62. [PubMed: 24892806]

19. Dhekne HS, Hsiao NH, Roelofs P, et al. Myosin Vb and Rab11a regulate phosphorylation of ezrin in enterocytes. J Cell Sci. 2014; 127:1007–17. [PubMed: 24413175]

20. Sato T, Mushiake S, Kato Y, et al. The Rab8 GTPase regulates apical protein localization in intestinal cells. Nature. 2007; 448:366–9. [PubMed: 17597763]

21. Pohl JF, Shub MD, Trevelline EE, et al. A cluster of microvillous inclusion disease in the Navajo population. J Pediatr. 1999; 134:103–6. [PubMed: 9880458]

22. Peng X-P, Yao X, Chow D-C, et al. Association of syntaxin 3 and vesicle associated membrane protein (VAMP) with H+/K+-ATPase-containing tubulovesicles in gastric parietal cells. Mol Biol Cell. 1997; 8:399–407. [PubMed: 9188093]

23. Calhoun BC, Goldenring JR. Two Rab proteins, vesicle-associated membrane protein 2 (VAMP-2) and secretory carrier membrane proteins (SCAMPs), are present on immunoisolated parietal cell tubulovesicles. Biochem J. 1997; 325(Pt 2):559–64. [PubMed: 9230141]

24. Roland JTE, Bryant DM, Datta A, et al. Rab GTPase-Myo5B complexes control membrane recycling and epithelial polarization. Proc Natl Acad Sci U S A. 2011; 108:2789–2794. [PubMed: 21282656]
25. Girard M, Lacaille F, Verkarre V, et al. MYO5B and bile salt export pump contribute to cholestatic liver disorder in microvillous inclusion disease. Hepatology. 2014; 60:301–10. [PubMed: 24375397]
26. Qiu YL, Gong JY, Feng JY, et al. Defects in MYO5B are associated with a spectrum of previously undiagnosed low gamma-glutamyltransferase cholestasis. Hepatology. 2016
27. Verghese E, Zhuang J, Saiti D, et al. In vitro investigation of renal epithelial injury suggests that primary cilium length is regulated by hypoxia-inducible mechanisms. Cell Biol Int. 2011; 35:909–13. [PubMed: 21241248]
28. Westlake CJ, Baye LM, Nachury MV, et al. Primary cilia membrane assembly is initiated by Rab11 and transport protein particle II (TRAPPII) complex-dependent trafficking of Rabin8 to the centrosome. Proc Natl Acad Sci U S A. 2011; 108:2759–64. [PubMed: 21273506]
29. Lapierre LA, Kumar R, Hales CM, et al. Myosin vb is associated with plasma membrane recycling systems. Mol Biol Cell. 2001; 12:1843–57. [PubMed: 11408590]
30. Nicol LE, O'Brien TD, Dumesic DA, et al. Abnormal infant islet morphology precedes insulin resistance in PCOS-like monkeys. PLoS One. 2014; 9:e106527. [PubMed: 25207967]
31. Oatman OJ, Djedjos CS, Olson ML, et al. Diabetes mellitus in microvillus inclusion disease. J Pediatr Gastroenterol Nutr. 2014; 59:e50–1. [PubMed: 23648791]
32. Westlake CJ, Junutula JR, Simon GC, et al. Identification of Rab11 as a small GTPase binding protein for the Evi5 oncogene. Proc Natl Acad Sci U S A. 2007; 104:1236–41. [PubMed: 17229837]
33. Nachury MV, Loktev AV, Zhang Q, et al. A core complex of BBS proteins cooperates with the GTPase Rab8 to promote ciliary membrane biogenesis. Cell. 2007; 129:1201–13. [PubMed: 17574030]
34. Roland JT, Kenworthy AK, Peranen J, et al. Myosin Vb Interacts with Rab8a on a Tubular Network Containing EHD1 and EHD3. Mol Biol Cell. 2007; 18:2828–2837. [PubMed: 17507647]
35. Wang J, Deretic D. The Arf and Rab11 effector FIP3 acts synergistically with ASAP1 to direct Rabin8 in ciliary receptor targeting. J Cell Sci. 2015; 128:1375–85. [PubMed: 25673879]
36. Vetter M, Wang J, Lorentzen E, et al. Novel topography of the Rab11-effector interaction network within a ciliary membrane targeting complex. Small GTPases. 2015; 6:165–73. [PubMed: 26399276]
37. Roland JT, Lapierre LA, Goldenring JR. Alternative splicing in class V myosins determines association with Rab10. J Biol Chem. 2009; 284:1213–23. [PubMed: 19008234]

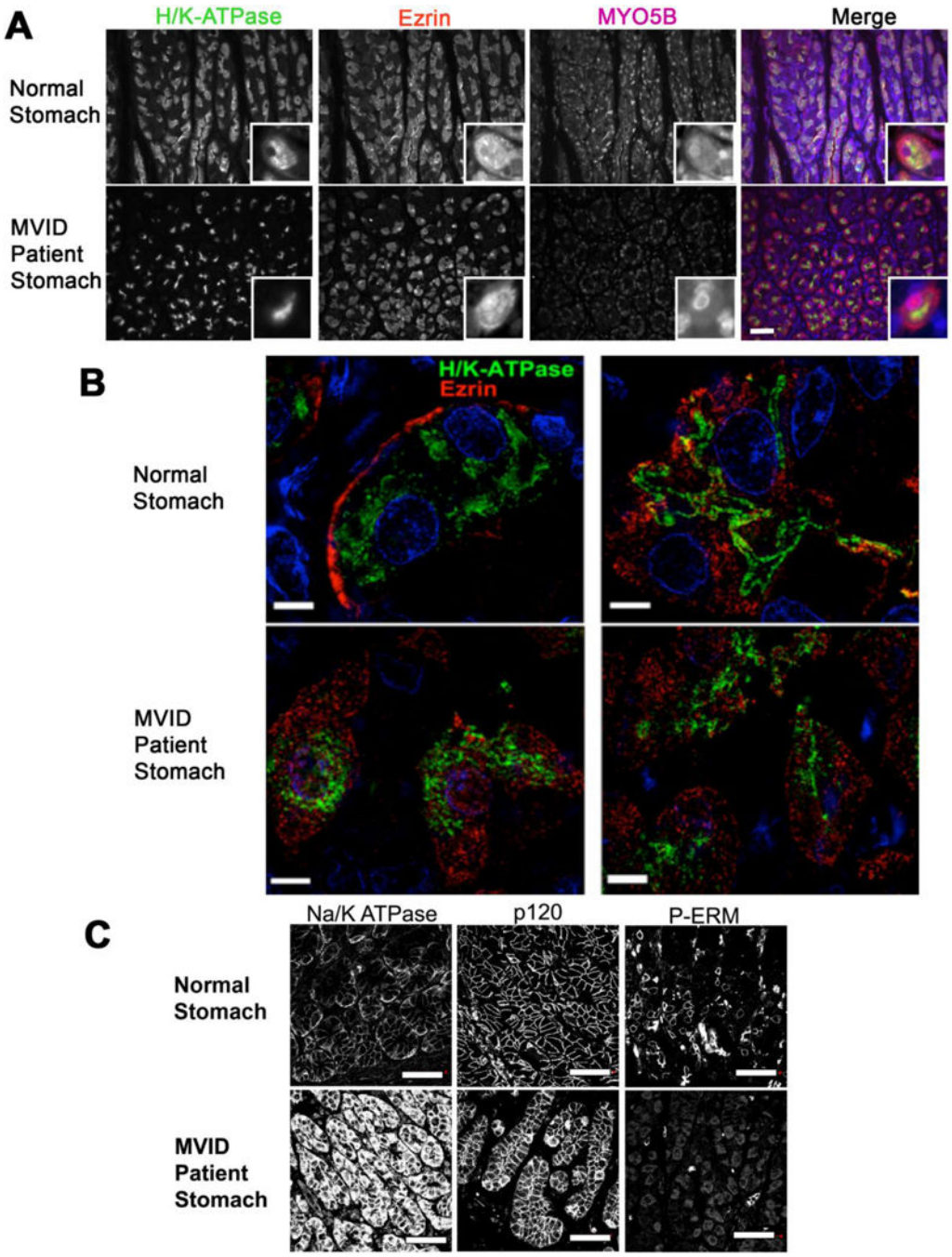

Figure 1. Immunostaining of Navajo MVID patient stomach samples loss loss of normal apical canalicular surfaces in parietal cells

(A) Sections of normal and MVID patient stomach were immunostained for H/K-ATPase (green), ezrin (red) and MYO5B (cyan). High magnification insets are shown in the lower right corners. Normal stomach showed a characteristic filigree pattern for ezrin staining of the intracellular canaliculus and H/K-ATPase staining of the subcanalicular tubulovesicles in parietal cells. MVID patient stomach immunostaining showed collapse and concentration of the tubulovesicular membrane staining for H/K-ATPase and a decrease in ezrin staining in parietal cells. (B) Structured Illumination Microscopy (SIM) imaging of H/K-ATPase and

ezrin staining in normal and MVID parietal cells. From the normal stomach, the images show parietal cells with normal resting pool of H/K-ATPase with H/K-ATPase distributed beneath the ezrin-staining canalicular surface. In the MVID patient samples parietal cells show an aberrant collapsed accumulation of intracellular H/K-ATPase and decreased ezrin staining. Contrast enhancements of SIM images were adjusted separately. (C) Sections of normal and MVID patient stomach were immunostained for Na/K-ATPase, p120 and phospho-ERM (P-ERM). In MVID patient samples, Na/K-ATPase, and p120 maintain normal basolateral localization, but have increased cytoplasmic localization. Phosphorylated-ERM staining, a reflection of ezrin phosphorylation in parietal cells, was markedly decreased in the MVID patient samples. Scale bars are 50 μm in all panels.

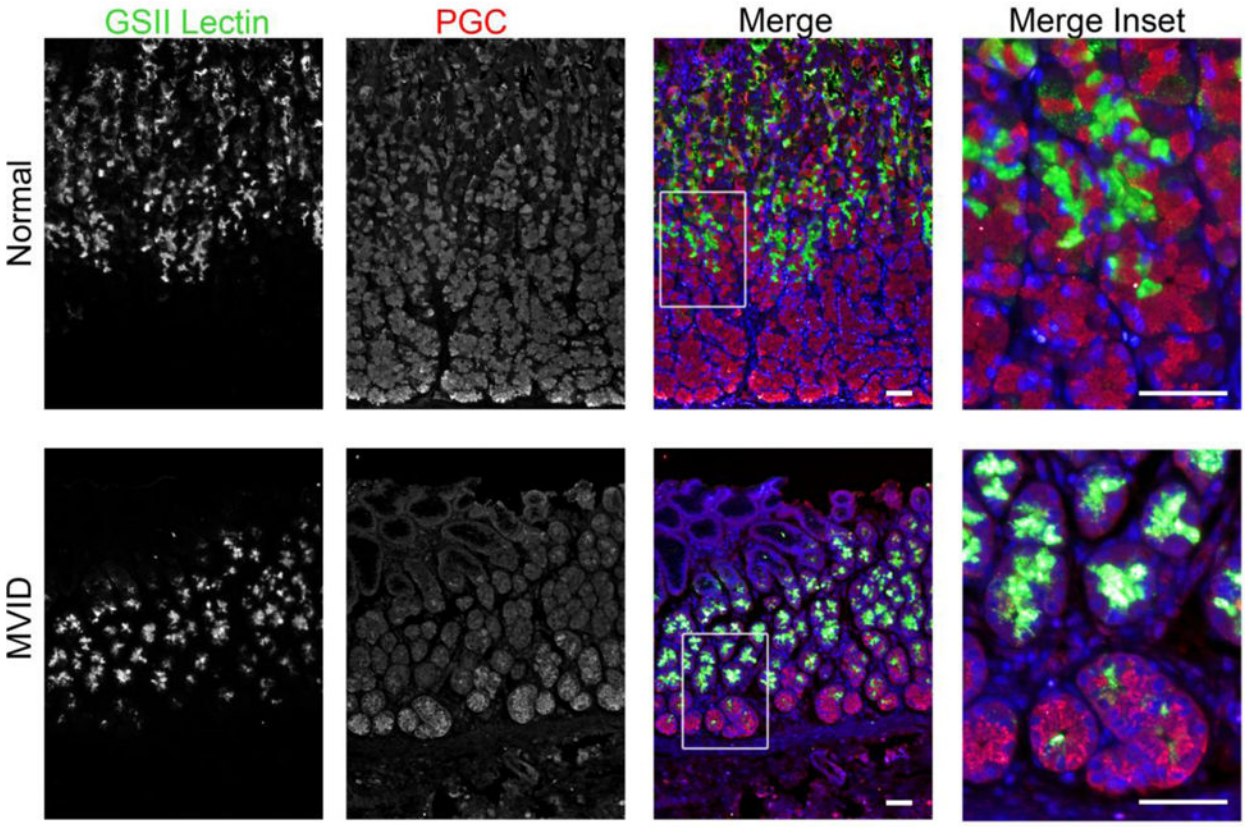

Figure 2. Immunostaining of Navajo MVID patient stomach shows normal morphologies in mucous neck cells and chief cells

Sections of normal and MVID patient stomach were stained with GSII lectin (green) and antibodies against pepsinogen (PGC-red) to visualize secretory granules in mucous neck cells and chief cells, respectively. Bar = 10 μm.

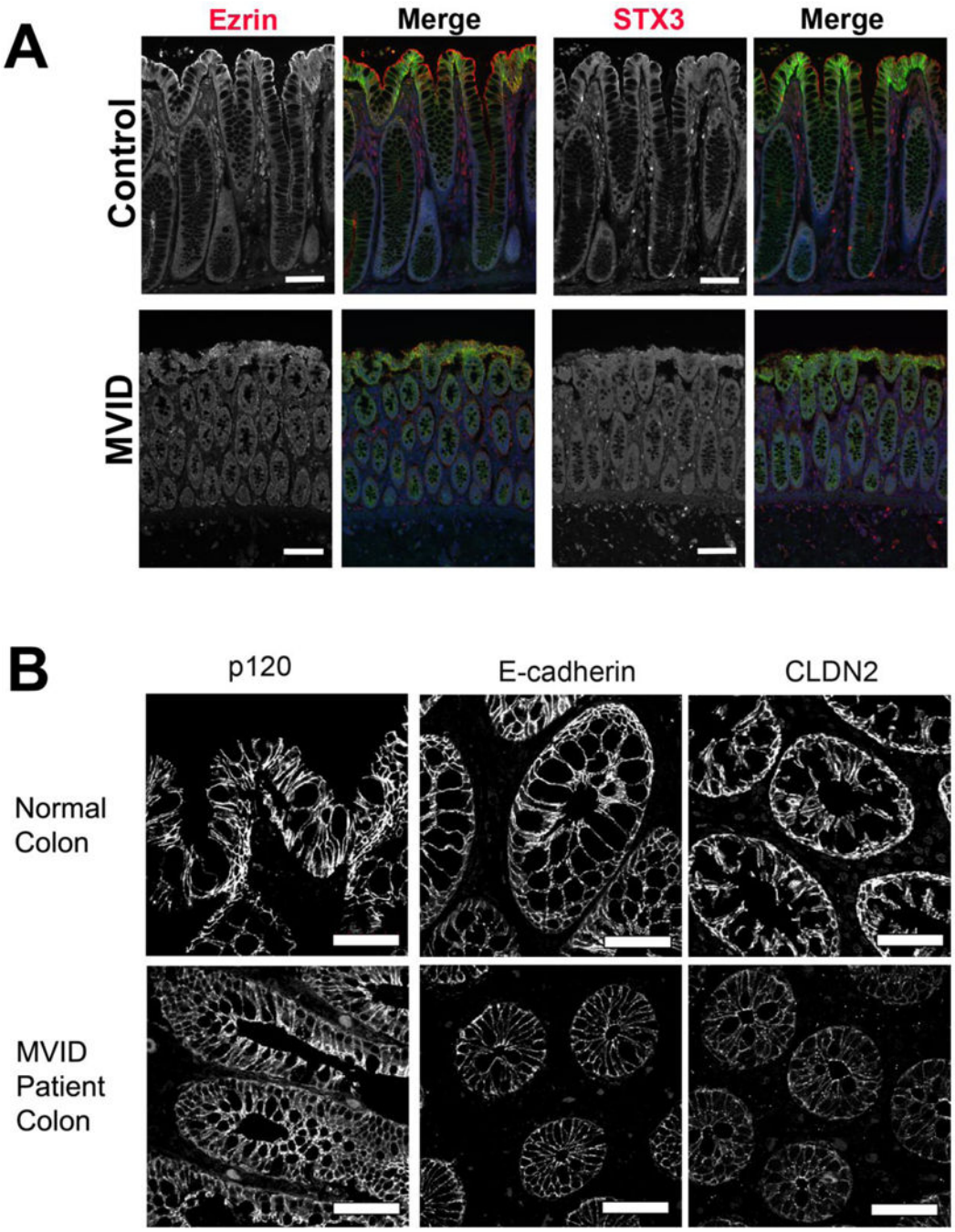

Figure 3. Alterations in apical membranes in MVID colonocytes

(A) Normal and MVID patient sections of colon were immunostained for Ezrin (red) or Syntaxin 3 (red) along with p120 (green) along with DAPI nuclear staining (blue). MVID patient colonocytes showed loss of apical staining of both Ezrin and Syntaxin 3. Scale bars = 100 μm. (B) Sections of normal and MVID patient colon were immunostained for p120, E-cadherin, or CLDN2. While levels of E-cadherin and Cldn2 appeared decreased they maintained a normal basolateral distribution. Scale bars = 50 μm.

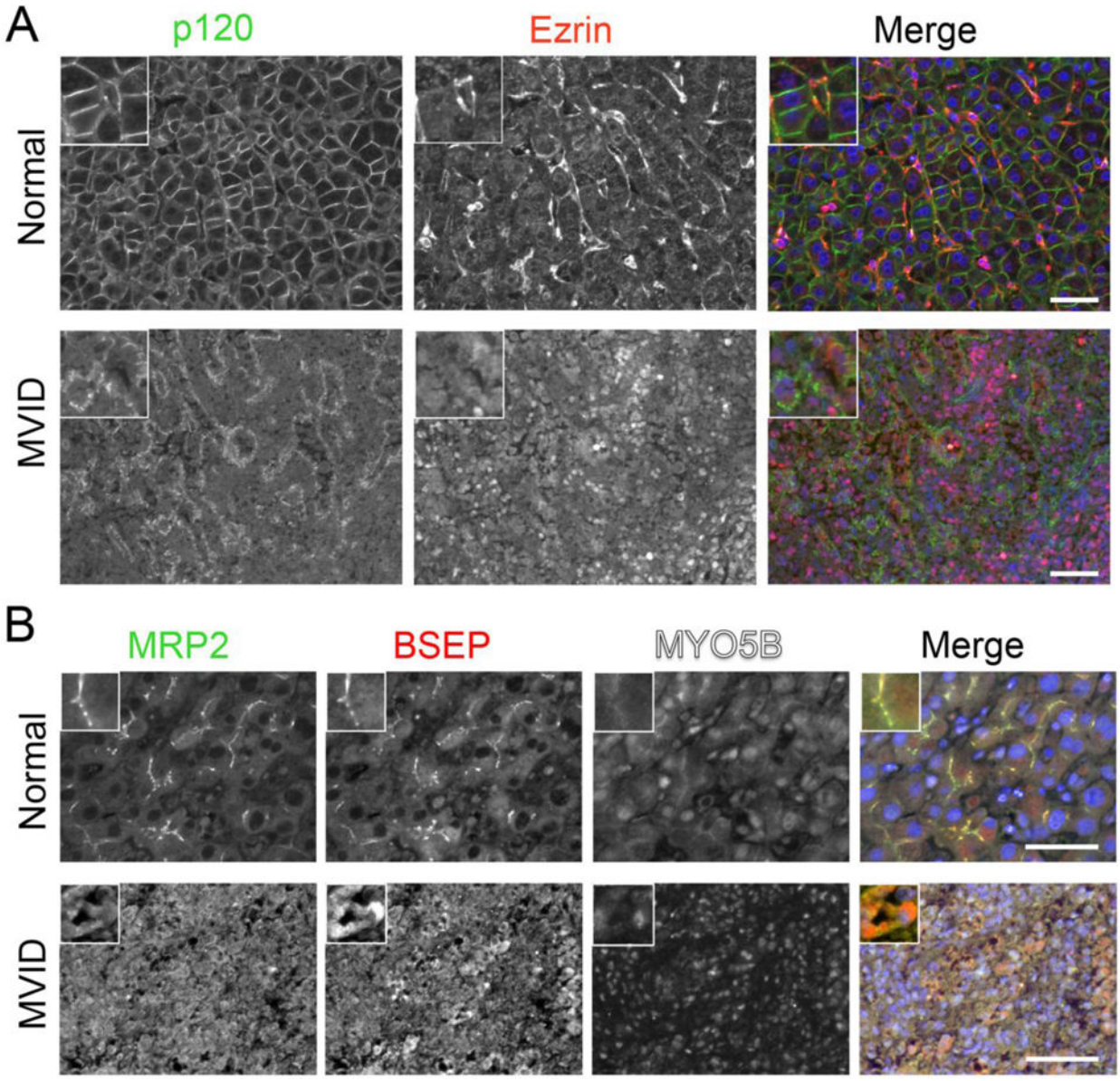

Figure 4. Immunostaining of MVID patient liver tissue samples shows redistribution of normal canalicular surface proteins

(A) Sections of normal and MVID patient liver were immunostained for p120 (green) and Ezrin (red) to label the sinusoidal and canalicular surfaces of hepatocytes, respectively, along with DAPI nuclear staining (blue). The p120 staining in MVID hepatocytes was redistributed into intracellular puncta, while ezrin was substantially lost from the canaliculi. (B) Sections of normal and MVID patient liver were immunostained for MRP2 (green), BSEP (red), and MYO5B (grayscale) along with DAPI nuclear staining (blue). In MVID patient liver, both MRP2 and BSEP staining was distributed aberrantly in the cytoplasm. Scale bars = 50 μm in all panels. Higher magnification insets are shown in the upper left of all panels.

Table 1

Antibodies used.

Antibody	Vendor	Dilution
Acetylated-tubulin	Sigma #T7451	1:2000
BSEP	Kamiya Biomedical #PC-064	1:200
Claudin-2	Invitrogen #51-6100	1:200
E-cadherin	BD Transduction Labs #610181	1:200
Ezrin	Cell Signaling #3145	1:5000
H/K-ATPase	Gift of Adam Smolka	1:200
Insulin		
MRP2	Enzo Life Sciences #M2111-6	1:200
Myo5B	Produced by Goldenring Lab	1:200
Na/K-ATPase	Millipore #05-369	1:50
P120	BD Transduction Labs #610133	1:200
Pepsinogen C (Pepsinogen II)	Abcam	1:1000
Phospho-ERM	Cell Signaling #3149	1:200
Syntaxin 3	Abcam #ab4113	1:200